Bioconjugate Chemistry

Article

pubs.acs.org/bc

Activatable Organic Near-Infrared Fluorescent Probes Based on a Bacteriochlorin Platform: Synthesis and Multicolor *in Vivo* Imaging with a Single Excitation

Toshiko Harada,[†] Kohei Sano,[†] Kazuhide Sato,[†] Rira Watanabe,[†] Zhanqian Yu,[‡] Hirofumi Hanaoka,[†] Takahito Nakajima,[†] Peter L. Choyke,[†] Marcin Ptaszek,[‡] and Hisataka Kobayashi*[,†]

[†]Molecular Imaging Program, Center for Cancer Research, National Cancer Institute, National Institutes of Health, Bethesda, Maryland 20892, United States

[‡]Department of Chemistry and Biochemistry, University of Maryland, Baltimore County, Baltimore, Maryland 21250, United States

Supporting Information

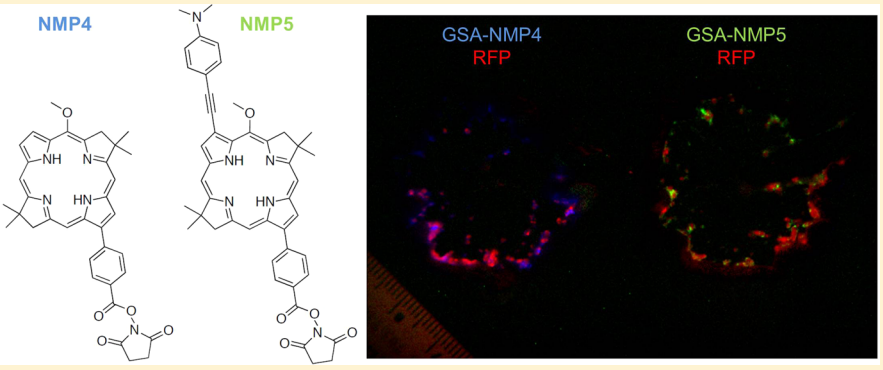

ABSTRACT: Near infrared (NIR) fluorescent probes are ideal for *in vivo* imaging because they offer deeper tissue penetration and lower background autofluorescence. Although most fluorophores in this range are cyanine-based dyes, several new classes of fluorescent NIR probes have been developed. In this study, we developed organic bacteriochlorin derivatives, NMP4 and NMP5, which are excited with a single green light and emit different narrow, well-resolved bands in the NIR (peak of 739 and 770 nm for NMP4 and NMP5, respectively). When conjugated to galactosyl-human serum albumin (hGSA) or glucosyl-human serum albumin (glu-HSA), both targeting H-type lectins, including the β-D-galactose receptor expressing on ovarian cancer, these agents become targeted, activatable, single excitation, multicolor NIR fluorescence probes. After conjugation to either glu-HSA or hGSA, substantial quenching of fluorescence occurs that is reversed after cell binding and internalization. *In vitro* studies showed higher cancer cell uptake with NMP4 or NMP5 conjugated to hGSA compared to the same conjugates with glu-HSA. *In vivo* single excitation two-color imaging was performed after intraperitoneal injection of these agents into mice with disseminated ovarian cancer. Excited with a single green light, distinct NIR emission spectra from each fluorophore were detected and could be distinguished with spectral unmixing. *In vivo* results using a red fluorescence protein (RFP) labeled tumor model of disseminated ovarian cancer demonstrated high sensitivity and specificity for all probes. The success of single excitation, 2-color NIR fluorescence imaging with a new class of bacteriochlorin-based activatable fluorophores, NMP4 and NMP5, paves the way for further exploration of noncyanine dye-based NIR fluorophores.

INTRODUCTION

Fluorescence molecular cancer imaging is gaining momentum as a method to assist surgeons and endoscopists to identify small foci of disease during procedures.[1,2] To date, most conventional optical imaging has relied on monochromatic, visible range, and "always on" contrast agents, which emit a single wavelength of light whether or not they are bound to the target. This approach suffers from high background signals and diminished sensitivity.[3−5] In contrast, activatable probes are turned on, only when they bind to their target resulting in much higher target-to-background ratios.

Although near-infrared (NIR) fluorescence emission is advantageous in *in vivo* fluorescence imaging due to superior light penetration and low autofluorescence from the biological tissue,[6,7] multichromatic NIR fluorescence imaging is more difficult to achieve than fluorescence imaging in the visible wavelength range because physical energy differences are smaller in the NIR range making color separation of each emission spectrum more difficult. A desirable property of

Received: November 7, 2013
Revised: January 21, 2014
Published: January 22, 2014

organic NIR fluorophores is that they are relatively small molecules to permit better biodistribution even after conjugating with targeting ligands. For instance, although quantum dots are highly efficient NIR fluorophores yielding multiple different emissions with a single excitation light and a large Stokes shift,[8] they are too large to label targeting moieties binding to specific molecules. However, in order to perform multichromatic NIR fluorescence imaging with conventional organic fluorophores, which have a small Stokes shift, a little complicated multi-excitation spectral technique should be employed using a special camera system with a special algorism for calculation.[9,10]

In this study, we describe two newly synthesized NIR fluorescence probes based on a bacteriochlorin platform, NMP4 and NMP5, which can be excited with a single green light but emits distinct wavelengths of NIR light with light strength similar to that of NIR quantum dots. When NMP4 and NMP5 were conjugated with galactosyl-human serum albumin (hGSA) or glucosyl-human serum albumin (glu-HSA), and the fluorophores were quenched until they were released and thereby activated after cellular internalization.

NMP4 and NMP5 are synthetic bacteriochlorin derivatives. Bacteriochlorins are tetrapyrrolic macrocycles, that constitute the core of the photosynthetic pigments in photosynthetic bacteria[11−13] and exhibit an intensive emission in the NIR spectral window (716−823 nm, with the quantum yields ranging from 0.04 to 0.25).[14] The emission band is relatively narrow (with full-width-at-half-maximum ranging from 17 to 26 nm), and the peak can be precisely tuned by a simple substitution on the macrocycle periphery.[14,15] Additionally, bacteriochlorins possess multiple excitation bands, including a band in the NIR (Q_y band between 710 and 820 nm) and a Q_x band in the visible range (green ∼510−530 nm). Taken together, bacteriochlorins possess a unique set of properties, which make them well suited for development as fluorophores with a single excitation wavelength in the green spectral window and narrow, well-resolved emission bands in NIR. Bacteriochlorins have been already reported for *in vivo* fluorescence[16−18] and photoacoustic imaging.[19] Herein, we describe and characterize a pair of synthetic bacteriochlorins that were used to detect peritoneal ovarian cancer metastases (POCM), which grew on the surface of the peritoneal membrane *in vivo*.

MATERIALS AND METHODS

Synthesis of Bacteriochlorins. *NMP4-NHS.* A mixture of NMP4-Me[20] (14 mg, 26 μmol), aqueous NaOH solution (2 mL, 2M), THF (4 mL), and methanol (2 mL) was stirred at room temperature for 12 h. HCl solution (10 mL, 1M) was added. The resulting mixture was extracted with ethyl acetate. Combined organic layers were washed with brine, dried (Na_2SO_4), and concentrated to afford a crude acid (19 mg, 100%). The resulting acid was treated with DMAP (12 mg, 100 μmol) and *N*-hydroxysuccinimide (30 mg, 261 μmol) in DMF (1 mL), followed by EDC (19 mg, 100 μmol). After 16 h, the mixture was diluted with ethyl acetate, washed with brine, dried (Na_2SO_4), and concentrated. The residue was purified with silica column chromatography (CH_2Cl_2/ ethyl acetate (25:1)) to give a green solid (11 mg, 68%). ^{1}H NMR ($CDCl_3$, 400 MHz) δ −2.14 (s, 1H), −1.92 (s, 1H), 1.96 (s, 6H), 1.99 (s, 6H), 2.98 (s, 4H), 4.41 (s, 2H), 4.43 (s, 2H), 4.50 (s, 3H), 8.34 (d, *J* = 8.6 Hz, 2H), 8.51 (d, *J* = 8.6 Hz, 2H), 8.68 (s, 1H), 8.71−8.74 (m, 2H), 8.82 (s, 1H), 8.85 (d, *J* = 2.4 Hz, 1H), 8.98 (dd, *J* = 1.8, 4.6 Hz, 1H); ^{13}C NMR ($CDCl_3$, 100 MHz) δ 25.8, 31.0, 31.1, 45.6, 45.8, 47.8, 51.7, 65.3, 96.4, 96.8, 97.3, 118.5, 121.4, 121.43, 123.4, 131.1, 131.3, 131.8, 133.2, 133.4, 134.4, 135.2, 136.5, 143.7, 154.5, 159.4, 162.1, 168.9, 169.4, 170.2. MS ($[M + H]^+$, M = $C_{36}H_{35}N_5O_5$): calcd, 618.2711; obsd, (MALDI-MS) 617.7, (HRMS, ESI) 618.2719 (Supporting Information, Figure 1).

NMP5-NHS. A mixture of NMP5-Me[20] (16.5 mg, 24 μmol), aqueous NaOH solution (2 mL, 2M), THF (4 mL), and methanol (2 mL) was stirred at room temperature for 15 h. HCl solution (4 mL, 1M) was added. The resulting mixture was extracted with ethyl acetate. Combined organic layers were washed with brine, dried (Na_2SO_4), and concentrated to afford a crude acid (16.0 mg, 99%). A solution of crude acid (8.1 mg, 12 μmol) was treated with DMAP (15 mg, 120 μmol) and *N*-hydroxysuccinimide (14 mg, 120 μmol) in DMF (1 mL), followed by EDC (23 mg, 120 μmol). The resulting mixture was stirred at room temperature. After 16 h, the resulting mixture was diluted with ethyl acetate, washed with brine, dried (Na_2SO_4), and concentrated. The residue was purified with silica column chromatography (CH_2Cl_2/ ethyl acetate (25:1)) to give a red-brown solid (4 mg, 43%). ^{1}H NMR ($CDCl_3$, 400 MHz) δ −1.87 (s, 1H), −1.51 (s, 1H), 1.94 (s, 6H), 1.97 (s, 6H), 2.99 (s, 4H), 3.08 (s, 6H), 4.36 (s, 2H), 4.47 (s, 2H), 4.51 (s, 3H), 6.82 (d, *J* = 8.6 Hz, 2H), 7.75 (d, *J* = 8.6 Hz, 2H), 8.32 (d, *J* = 8.0 Hz, 2H), 8.50 (d, *J* = 7.9 Hz, 2H), 8.55 (s, 1H), 8.64 (s, 1H), 8.72 (s, 1H), 8.78 (d, *J* = 1.8 Hz, 1H), 8.81 (d, *J* = 1.2 Hz, 1H); ^{13}C NMR ($CDCl_3$, 100 MHz) δ 25.7, 30.9, 31.0, 40.3, 45.6, 47.6, 51.8, 64.5, 85.2, 95.3, 96.4, 96.7, 97.4, 111.1, 112.0, 114.0, 122.9, 123.5, 124.2, 131.1, 131.2, 131.4, 132.9, 133.8, 134.4, 134.8, 135.0, 135.5, 143.3, 150.1, 155.2, 160.6, 162.0, 169.3, 169.7, 169.9; MS ($[M + H]^+$, M = $C_{46}H_{44}N_6O_5$): calcd, 761.3446; obsd, (MALDI-MS) 761.3, (HRMS, ESI) 761.3445 (Supporting Information, Figure 2).

Synthesis, Chemical Activation, and Stability in Serum of hGSA-NMP Conjugates. hGSA (250 μg, 3.5 nmol) or glu-HSA (250 μg, 3.5 nmol) were incubated with the NMP4-NHS ester (21.6 μg, 35 nmol) or NMP5-NHS ester (26.7 μg, 35 nmol) in 0.1 M Na_2HPO_4 (pH8.6) at room temperature for 1 h, followed by purification with a size exclusion column (PD-10; GE Healthcare, Piscataway, NJ). The concentrations of each dye in the sample solution were calculated based on maximum extinction coefficient values of NMP4 and NMP5, which are 96,000 L/mol/cm at 735 nm and 99,000 L/mol/cm at 762 nm, respectively, by measuring the absorption with a UV−vis system (8453 Value UV−vis system; Agilent Technologies, Santa Clara, CA) using 1-cm width of cuvettes. The protein concentration was also determined by measuring the absorption at 280 nm with a UV−vis system. The number of fluorophore molecules conjugated with each hGSA or glu-HSA molecule was confirmed by dividing the dye concentration by the protein concentration.

The quenching abilities of each conjugate were investigated by denaturing each with 1% SDS as described previously.[21,22] Briefly, the conjugates were incubated either with 1% SDS in PBS or PBS alone for 15 min at room temperature. The change in fluorescence intensity of NMP4 and NMP5 was investigated with an *in vivo* imaging system (Maestro, CRi Inc., Woburn, MA) using the following filter set: 503−555 nm for excitation light and long-pass filter over 700 or 750 nm for emission light.

Each probe was added to mouse serum collected from female nude mice (National Cancer Institute Animal Production Facility, Frederick, MD), and the serum samples were incubated at 37 °C for 0, 0.5, 1, and 1.5 h. After incubation,

dx.doi.org/10.1021/bc4005238 | *Bioconjugate Chem.* 2014, 25, 362−369

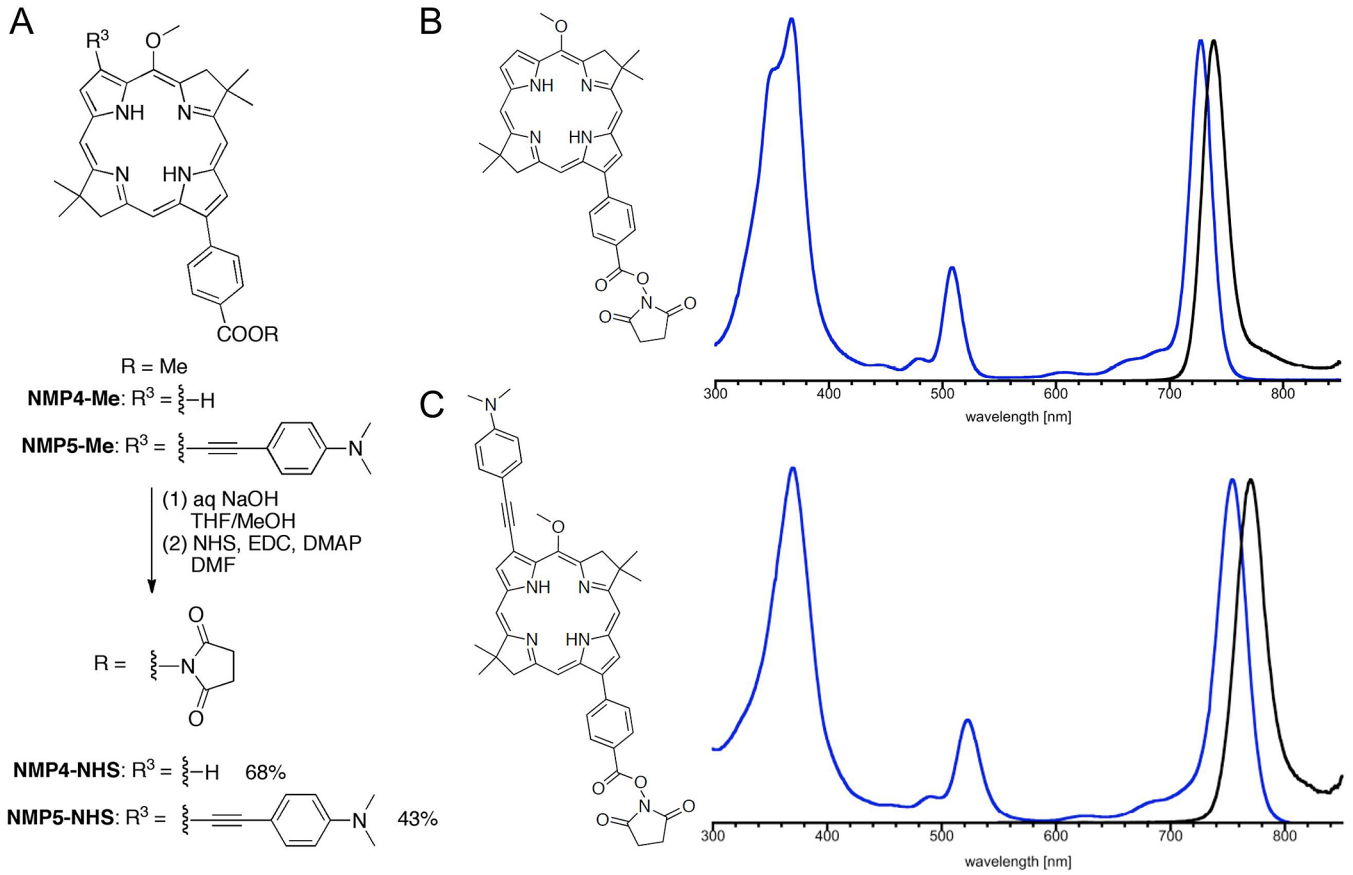

Figure 1. Synthesis of NMP4-NHS and NMP5-NHS (A). Chemical structures of the NMP4-NHS ester (B) and the NMP5-NHS ester (C) and their absorption (blue line) and emission (black line) profiles. Both dyes have two available excitation peaks in green and NIR wavelengths and yield NIR emission (739 and 770 nm for NMP4 and NMP5 in dimethylsulfoxide, respectively) by exciting green or NIR light.

the change in fluorescence intensity was evaluated with a Maestro camera.

Cell Culture. The established ovarian cancer cell line, SHIN3, was used for *in vitro* fluorescence microscopy and *in vivo* optical imaging of POCM. SHIN3 DsRed, in which the red fluorescent protein (RFP DsRed2)-expressing plasmid (Clontech Laboratories) was previously transfected, served as the standard of reference for cancer location.[33] Cell lines were grown in RPMI 1640 medium (Invitrogen) containing 10% fetal bovine serum (Gibco), 0.03% L-glutamine at 37 °C, 100 U/mL penicillin, and 100 μg/mL streptomycin in 5% CO_2.

Fluorescence Microscopy Studies. SHIN3 cells (1×10^4) were plated on a cover glass bottomed culture well and incubated for 16 h. hGSA-NMP4, hGSA-NMP5, glu-HSA-NMP4, and glu-HSA-NMP5 were then added at 1 μg/mL. The cells were incubated for either 1 or 8 h followed by washing once with PBS, and fluorescence microscopy was performed using an Olympus BX61 microscope (Olympus America, Inc., Melville, NY) equipped with the following filters: excitation wavelength 672.5–747.5 nm and emission wavelength range 765–855 nm. Transmitted light differential interference contrast (DIC) images were obtained as well. To validate the specific binding of the probe, 100 μg of nonconjugated hGSA of glu-HSA was added to block 1 μg of conjugates.

Animal Model of Peritoneal Metastases. All procedures were carried out in compliance with the Guide for the Care and Use of Laboratory Animal Resources (1996), US National Research Council, and were approved by the local Animal Care and Use Committee. Six to eight-week-old female homozygote athymic nude mice were purchased from Charles River (National Cancer Institute, Frederick, MD). Intraperitoneal xenografts were established by i.p. injection of 2×10^6 SHIN3 cells suspended in 200 μL of PBS into the peritoneal cavity of nude mice. Imaging was performed at 14–21 days after injection of the cells.

***In Vivo* Activatable Imaging.** A mixture of (i) hGSA-NMP4 and glu-HSA-NMP5 or (ii) hGSA-NMP5 and glu-HSA-NMP4 (each 25 μg) was injected into the peritoneal cavities of SHIN3 tumor bearing mice ($n \geq 3$ for each group). Mice were euthanized by carbon dioxide inhalation 1 h after the i.p. injection of each probe. After euthanasia, the mouse abdominal wall was excised, and the abdominal cavity was exposed. Optical images of the whole abdomen were first obtained. Following this, the small bowel mesentery was extracted, and close-up images were obtained. Spectral fluorescence images were acquired using the Maestro *In-Vivo* Imaging System. The following filter set was used for imaging NMP4 and NMP5: a band-pass filter from 503 to 555 nm for excitation light and a long-pass filter over 700 nm for emission light. The tunable emission filter was automatically stepped in 10 nm increments from 650 to 950 nm at constant exposure to generate a spectral image. The spectral fluorescence images consist of autofluorescence spectra and the spectra from NMP4 and NMP5, which were then unmixed, based on their spectral patterns using commercial software (Maestro software; CRi).

Assessment of Sensitivity and Specificity of hGSA-NMP4 and hGSA-NMP5 in the Detection of Peritoneal Metastases. To examine the sensitivity and specificity of

dx.doi.org/10.1021/bc4005238 | *Bioconjugate Chem.* 2014, 25, 362–369

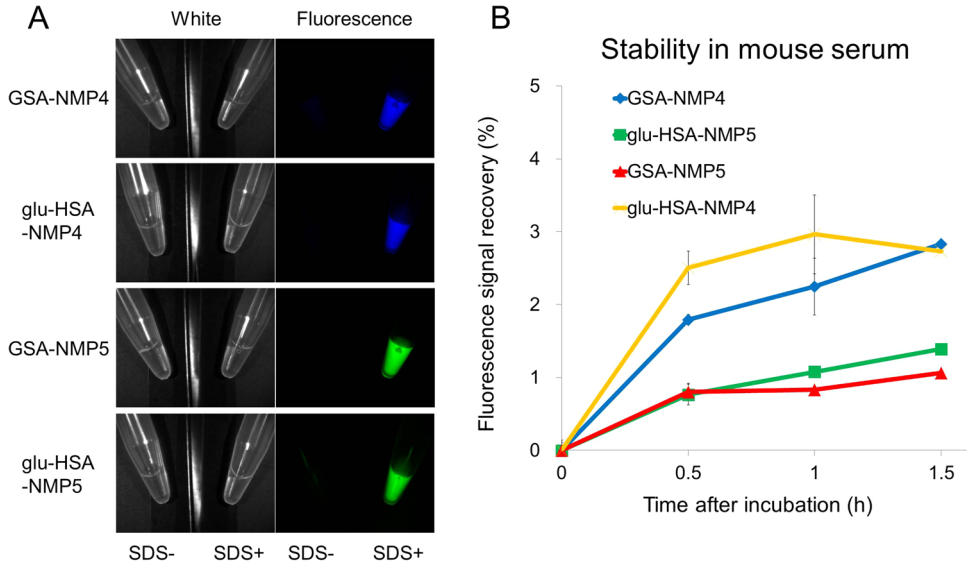

Figure 2. (A) Fluorescence signals of probes synthesized in this study with or without chemical activation by adding 1% SDS. All probes showed high activation ratios (more than 100). (B) Stability of probes in mouse serum. Fluorescence recovery was calculated by the following equation: (fluorescence signal in mouse serum − fluorescence signal in PBS)/(fluorescence signal in SDS/PBS − fluorescence signal in PBS) × 100. Data are presented as mean ± SEM. Each probe exhibited high stability in mouse serum for 1.5 h.

hGSA-NMP4 and hGSA-NMP5 for imaging peritoneal disseminated cancer foci, hGSA-NMP4 or hGSA-NMP5 (each 25 μg) was injected into the peritoneal cavities of RFP-transfected SHIN3 tumor bearing mice ($n \geq 3$ for each group). Mice were euthanized with carbon dioxide 1.5 h after i.p. injection of each probe. After euthanasia, the abdominal walls were exposed and were placed side by side on a nonfluorescent plate. Whole abdominal images as well as close-up images of the small bowel mesenteries were obtained. The small bowel mesenteries were extracted and spread out side by side on the nonfluorescent plate. Spectral fluorescence images were acquired using the Maestro camera. The following filter set was used: a band-pass filter from 503 to 555 nm for excitation light and two filters over 645 and 700 nm for emission light. The tunable emission filter was automatically stepped in 10 nm increments from 600 to 900 nm at constant exposure. The spectral fluorescence images consisting of spectra from RFP, NMP4, and NMP5 were then unmixed so that individual images of each channel were obtained.

Sensitivity and specificity were determined by comparing sites of fluorescence from hGSA-NMP4 and hGSA-NMP5 with sites of fluorescence from RFP-transfected SHIN3 tumors. The spectral fluorescence images were unmixed, and regions of interest (ROI) were assigned using automated software based on a predetermined threshold. Only nodules with short axis diameters >0.8 mm were included for analysis. RFP-positive nodules were defined as having an average fluorescence intensity >25 a.u. on images unmixed for the RFP spectra. True positives for hGSA-NMP4 and hGSA-NMP5 were defined as ROIs with an average fluorescence intensity of >3 a.u, whereas true negatives for hGSA-NMP4 and hGSA-NMP5 were defined as ROIs with an average fluorescence intensity <3 a.u. on the spectrally unmixed images. False positives for hGSA-NMP4 and hGSA-NMP5 were defined as ROIs in which fluorescence was seen only on the NMP4 or NMP5 image and not on the RFP image.

RESULTS

Synthesis. Several bioconjugatable bacteriochlorin derivatives have been reported previously.[20,23−27] The synthesis of NMP4-NHS and NMP5-NHS, which include a bioconjugatable *N*-hydroxysuccinimide moiety, is outlined in Figure 1A. The synthesis of the requisite methyl esters NMP4-Me and NMP5-Me was achieved by regioselective palladium-catalyzed derivatization of corresponding dibromobacteriochlorin and has been reported previously.[20] The methyl esters in NMP4-Me and NMP5-Me were hydrolyzed (2 M aqueous NaOH, in THF/MeOH) to provide the corresponding crude acid. TLC analysis showed complete consumption of the starting material and essentially the quantitative formation of the acids. The crude acids were reacted with *N*-hydroxysuccinimide in the presence of EDC and DMAP, in DMF,[20] to provide NMP4-NHS and NMP5-NHS in 68% and 43% yields, respectively.

Optical Characteristics of NMP4 or NMP5 Conjugated Probes. NMP4 and NMP5 have absorption spectra, typical for bacteriochlorin derivatives.[14,20] Thus, in DMSO NMP4-NHS and NMP5-NHS exhibit strong *B* bands in UV (368 and 370 nm), a Q_x band in the green range (509 and 523 nm), and a Q_y band in the NIR range (727 and 753 nm). The molar extinction coefficients were determined in DMSO and for NMP4-NHS are 1.2×10^5 $cm^{-1}{\cdot}M^{-1}$ (367 nm), 3.5×10^4 $cm^{-1}{\cdot}M^{-1}$ (509 nm), and 9.6×10^4 $cm^{-1}{\cdot}M^{-1}$ (727 nm), and for NMP5-NHS are 1.1×10^5 $cm^{-1}{\cdot}M^{-1}$ (370 nm), 3.1×10^4 $cm^{-1}{\cdot}M^{-1}$ (523 nm), and 9.9×10^4 $cm^{-1}{\cdot}M^{-1}$ (753 nm). The absorption features of bacteriochlorins arise from the multiple $\pi-\pi^*$ transitions and can be explained on the basis of the four-orbital Gouterman's model, which was previously discussed in detail (see ref 14 and references cited therein). Both NMP4 and NMP5 emit at a NIR peak of 739 and 770 nm, respectively, regardless of the wavelength of excitation (Figure 1C). The quantum yields were previously determined for NMP4-Me and NMP5-Me are 0.22 and 0.20 (NMP4-Me), and 0.25 and 0.21 (NMP5-Me), in toluene and DMF, respectively.[20] The number of NMP4 and NMP5 dyes conjugated with hGSA and glu-HSA was 2.5 ± 0.4, 2.3 ± 0.3, 2.9 ± 0.2, and 2.3 ± 0.3 for hGSA-

dx.doi.org/10.1021/bc4005238 | *Bioconjugate Chem.* 2014, 25, 362−369

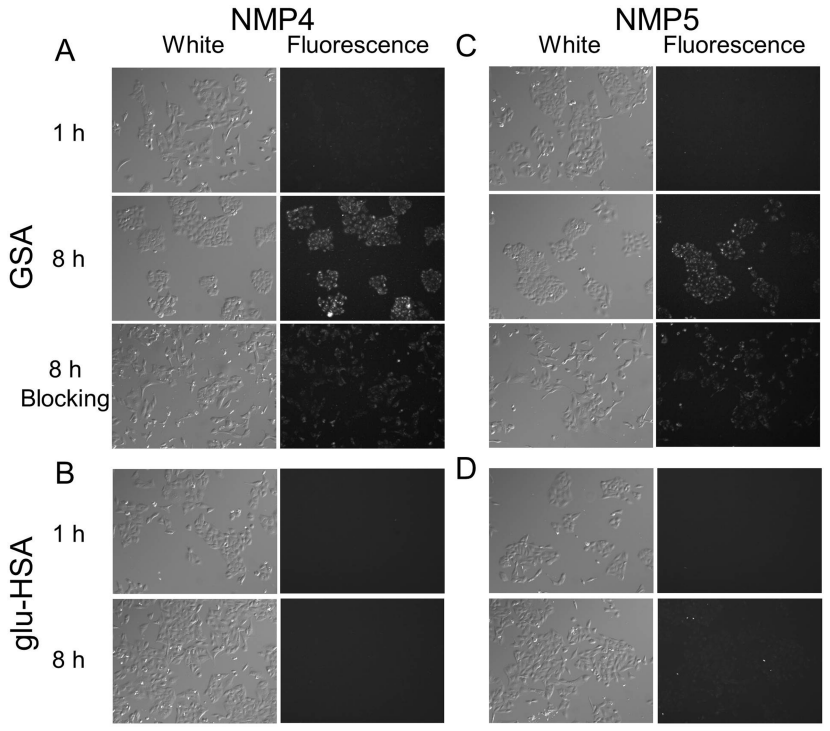

Figure 3. Fluorescence microscopy studies. SHIN3 cells were incubated with hGSA-NMP4, hGSA-NMP5, glu-HSA-NMP4, and glu-HSA-NMP5 for 1 and 8 h. Although hGSA-NMP4 and hGSA-NMP5 minimally accumulated in SHIN3 cells at 1 h, many bright spots were seen within SHIN3 cells after 8 h of incubation, which was partially blocked by excess hGSA. The accumulation of glu-HSA-NMP4 and glu-HSA-NMP5 was lower than that of hGSA conjugates.

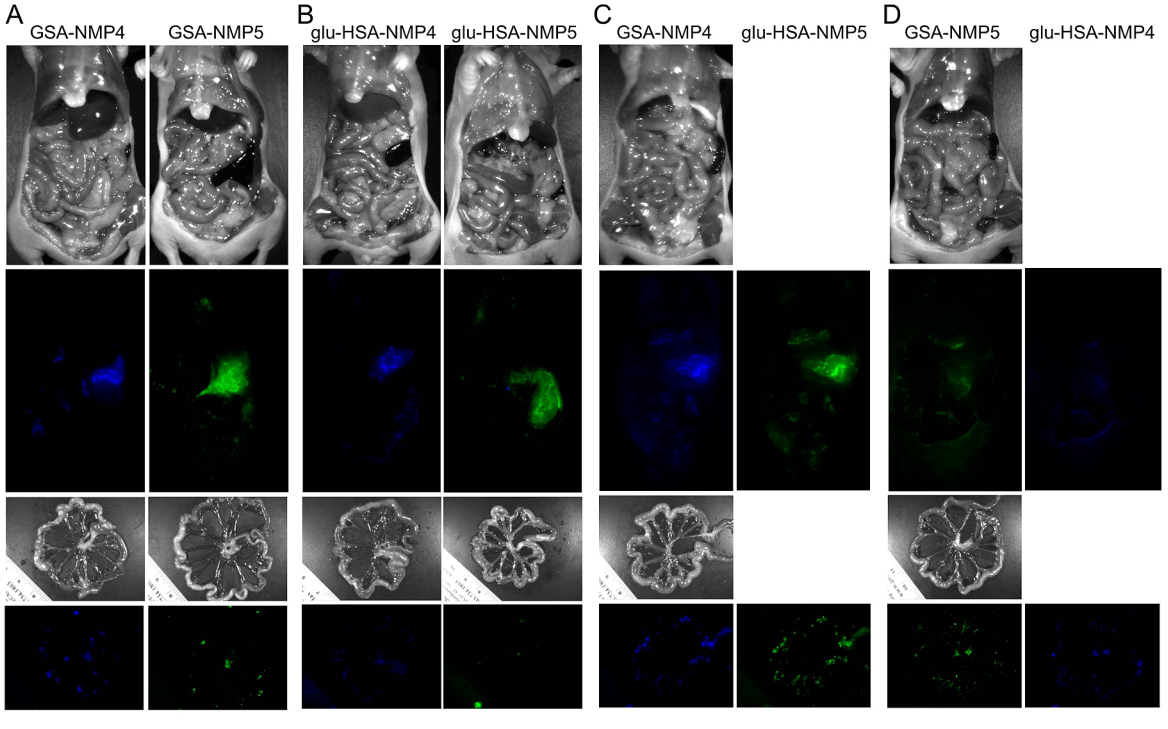

Figure 4. (A) Side-by-side images of SHIN3 tumor bearing mice i.p. administered with hGSA-NMP4 or hGSA-NMP5. The fluorescence signal of NMP4 (blue) and NMP5 (green) was unmixed with their spectral library. Both probes clearly visualized SHIN3 tumors *in vivo* in the mesentery with minimal background signal. (B) Side-by-side images of SHIN3 tumor bearing mice i.p. injected with glu-HSA-NMP4 and glu-HSA-NMP5. (C) A mixture of hGSA-NMP4 and glu-HSA-NMP5 was injected i.p. into SHIN3 tumor bearing mice. The fluorescence signals derived from NMP4 and NMP5 colocalized with the tumor in the mesentery. (D) A mixture of hGSA-NMP5 and glu-HSA-NMP4 was injected i.p. into SHIN3 tumor bearing mice.

dx.doi.org/10.1021/bc4005238 | *Bioconjugate Chem.* 2014, 25, 362−369

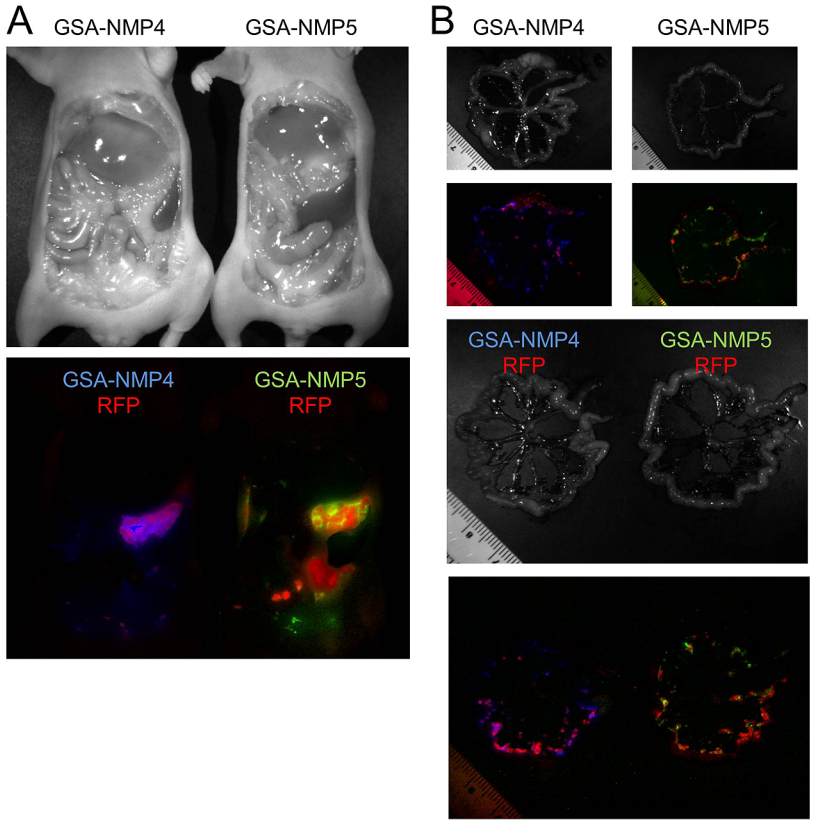

Figure 5. (A) Side-by-side images of RFP-transfected SHIN3 tumor bearing mice injected i.p. with hGSA-NMP4 or hGSA-NMP5. The fluorescence signals of RFP (red), NMP4 (blue), and NMP5 (green) were unmixed with their spectral library. Each probe clearly visualized RFP-transfected SHIN3 tumors. (B) Side-by-side images of extracted mesenteries of mice with RFP-transfected SHIN3 foci and previously injected hGSA-NMP4 or hGSA-NMP5. Fluorescence signals of RFP (red), NMP4 (blue), and NMP5 (green) are mostly coincident. Sensitivity and specificity of hGSA-NMP4 and hGSA-NMP5 for detecting RFP-transfected SHIN3 foci were calculated by examining 278 and 389 nodules, respectively.

NMP4, hGSA-NMP5, glu-HSA-NMP4, and glu-HSA-NMP5, respectively. The quenching capacities measured by adding 1% SDS to each probe were more than 100 for all probes (Figure 2A). Since the absorbance spectra of hGSA-NMP4, hGSA-NMP5, glu-HSA-NMP4, and glu-HSA-NMP5 were identical before and after dequenching with 1% SDS (Supporting Information, Figure 3), fluorescence signals of these agents were most likely quenched based on the fluorescence resonance energy transfer (FRET) mechanism. No measurable dequenching (~5%) of each probe was observed in mouse serum at 37 °C for 1.5 h (Figure 2B), demonstrating high *in vivo* stability.

***In Vitro* Fluorescent Characterization of Probes.** In the microscopy studies (Figure 3), many bright intracellular foci were present after 8 h of incubation with hGSA-NMP4 and hGSA-NMP5, while the signal was minimal at 1 h after incubation because of the robust quenching magnitude. These signals were partially blocked by the addition of excess hGSA. However, a low signal was detected in SHIN3 cells for glu-HSA-NMP4 and glu-HSA-NMP5 even after 8 h of incubation.

***In Vivo* Dual Probe Activatable Imaging.** hGSA-NMP4 or hGSA-NMP5 was injected into the peritoneal cavities of SHIN3 tumor bearing mice. The side-by-side images of hGSA-NMP4 and hGSA-NMP5 showed that the fluorescence signals can be distinguished *in vivo* by spectral unmixing with the fluorescence pattern of NMP4 and NMP5 (Figure 4A). Although similar results were obtained using glu-HSA-NMP4 and glu-HSA-NMP5, the signal intensities were lower than hGSA-based probes (Figure 4B), which was consistent with our previous data [28]

Upon administration of the mixture of hGSA-NMP4 and glu-HSA-NMP5, the colocalization of fluorescence signal derived from NMP4 and NMP5 was observed (Figure 4C).

Sensitivity and Specificity of hGSA-NMP4 and hGSA-NMP5. The side-by-side whole abdominal images of RFP-transfected SHIN3 cells with hGSA-NMP4 and with hGSA-NMP5 showed that the fluorescence signals can be distinguished *in vivo* by spectral acquisition and unmixing with a resulting fluorescence pattern of RFP, NMP4, and NMP5 (Figure 5A). The side-by-side mesenteric images of RFP-transfected SHIN3 cells with hGSA-NMP4 and with hGSA-NMP5 demonstrated that NMP4 and NMP5 were mostly coincident with RFP positive foci. The sensitivity and specificity of hGSA-NMP4 and hGSA-NMP5 for detecting SHIN3-DsRed tumors are depicted in Figure 5B. Sixty-six foci showed hGSA-NMP4 fluorescence among the 94 RFP-positive foci, while 20 foci showed hGSA-NMP4 fluorescence with intensity >3 a.u. among the 178 RFP-negative foci. Thus, hGSA-NMP4 was found to have a sensitivity of 70.2% (66 out of 94) and a specificity of 89.9% (158 out of 178). Ninety-five foci showed hGSA-NMP5 fluorescence among the 132 RFP-positive foci. Eleven foci showed hGSA-NMP4 fluorescence with intensity >3 a.u. among the 257 RFP-negative foci. Thus, hGSA-NMP5 was found to have a sensitivity of 72.0% (95 out of 132) and a specificity of 95.9% (246 out of 257).

dx.doi.org/10.1021/bc4005238 | *Bioconjugate Chem.* 2014, 25, 362−369

DISCUSSION

We investigated optical probes targeted to POCM using the glycoprotein, avidin, [29] a ligand for lectins similar to the β-D-galactose receptor, which is generally considered an "H-type" lectin. Unfortunately, since avidin is a hen egg protein, its immunogenicity precludes its clinical use. Seeking alternative lectin-targeted moieties, we subsequently conjugated green fluorescent dyes, like rhodamine green, to a nonimmunogenic ligand, hGSA.[30] The hGSA component is highly biocompatible and binds ovarian cancer with high specificity when administered intraperitoneally. Furthermore, the D-galactose receptor is an optimal target for other peritoneal metastases since it is expressed in a wide range of metastatic cancers.[31] In addition, hGSA has already been used in Japan as a clinical diagnostic agent in humans for measuring hepatic reserve. A fluorescent probe based on glu-HSA is a good control molecule since it does not bind to the D-galactose receptor as well as hGSA. This is because glu-HSA was synthesized with direct amidation using human serum albumin conjugated with the same number of glucosamines. Therefore, it is completely expected that the fluorescent glu-HSA probe showed minimal binding to the D-galactose receptor expressing SHIN3 cells *in vitro* (Figure 3). However, fluorescence- and radio-labeled glu-HSA probes showed binding to inflammatory cells associated with tumor implants *in vivo*[32] and accumulated significantly less in both SHIN3 tumors and the liver than hGSA-based probes (see also Supporting Information, Figure 4).

We demonstrate that it is feasible to image ovarian cancers with NMP4 and NMP5, representing a new class of NIR fluorophores, when they are conjugated with hGSA. Both fluorophores are quenched when conjugated with either hGSA or glu-HSA and showed high activation ratios (>100) after adding SDS or internalizing into the lysosome *in vitro*. Therefore, these probes allowed us to achieve *in vivo* fluorescence imaging with low background signal at earlier times (1.5 h) after injection compared with conventional "always on" fluorescence probes.[28,33]

Both NMP4 and NMP5 are chemically different from NMP-1, which we reported in our previous work.[34] For instance, NMP-1 has an entirely different emission spectrum compared to those of NMP4 and NMP5. This class of bacteriochlorin fluorophores can be highly tuned with regard to its NIR emission spectra making it unique in comparison to cyanine dyes. Therefore, with NMP-1, NMP4, and NMP5, we could theoretically perform 3-color NIR fluorescence imaging. However, since the current spectral camera is not sensitive enough to separate two distinct spectra with single nanometer difference in the range from 700 to 800 nm, we could successfully separate only NMP4 and NMP5 and show them in two colors. This low camera sensitivity in the NIR range technically led to low sensitivity for detecting tumor lesions because small photon numbers decreased NMP4 or NMP5 signals of tumor nodules after spectral separation from highly sensitive RFP.

Another advantage of bacteriochlorin-based fluorophores over conventional organic dyes is that all these probes can be excited with a single green light, which is completely separate from NIR emissions, thus minimizing the usual background autofluorescence seen with shorter Stokes shifts. Since bacteriochlorin-based fluorophores have quite sharp emission spectra, it should be possible to deliver a cocktail of 3 or more distinctly targeted probe conjugates to measure multiple receptors simultaneously all with a single excitation. Improvements in optical engineering will undoubtedly advance to the point where a single excitation can result in activation of 3 or more NIR peaks that can be separately resolved.

In conclusion, we describe a new activatable, multichromatic pair of fluorophores, NMP4 and NMP5, which are based on bacteriochlorin. We successfully performed single excitation, 2-color NIR fluorescence imaging *in vivo*. On the basis of the flexibility of bacteriochlorin-based chemistry, it should be possible to synthesize additional distinct fluorophores with slightly different emissions. With anticipated advances in optical engineering, bacteriochlorin-based fluorophores will allow us to perform a single excitation, multicolor NIR fluorescence imaging that could show multiple distinct parameters utilizing much smaller molecules than is possible with quantum dots.

ASSOCIATED CONTENT

Supporting Information

NMR spectra of fluorescent dyes and absorbance spectra and biodistribution of In-111 labeled hGSA and glu-HSA probes in normal and tumor bearing mice. This material is available free of charge via the Internet at http://pubs.acs.org.

AUTHOR INFORMATION

Corresponding Author

*Molecular Imaging Program, Center for Cancer Research, National Cancer Institute, NIH, Building 10, Room B3B69, MSC1088, Bethesda, MD 20892-1088. Phone: 301-435-4086. Fax: 301-402-3191. E-mail: kobayash@mail.nih.gov.

Notes

The authors declare no competing financial interest.

ACKNOWLEDGMENTS

This research was supported by the Intramural Research Program of the National Institutes of Health, National Cancer Institute, Center for Cancer Research. M.P. was supported by University of Maryland, Baltimore County (start-up funds and SRAIS Award).

REFERENCES

(1) Keereweer, S., Kerrebijn, J. D., van Driel, P. B., Xie, B., Kaijzel, E. L., Snoeks, T. J., Que, I., Hutteman, M., van der Vorst, J. R., Mieog, J. S., Vahrmeijer, A. L., van de Velde, C. J., Baatenburg de Jong, R. J., and Lowik, C. W. (2011) Optical image-guided surgery–where do we stand? *Mol. Imaging Biol. 13*, 199−207.

(2) van Dam, G. M., Themelis, G., Crane, L. M., Harlaar, N. J., Pleijhuis, R. G., Kelder, W., Sarantopoulos, A., de Jong, J. S., Arts, H. J., van der Zee, A. G., Bart, J., Low, P. S., and Ntziachristos, V. (2011) Intraoperative tumor-specific fluorescence imaging in ovarian cancer by folate receptor-alpha targeting: first in-human results. *Nat. Med. 17*, 1315−1319.

(3) Kobayashi, H., and Choyke, P. L. (2011) Target-cancer-cell-specific activatable fluorescence imaging probes: rational design and in vivo applications. *Acc. Chem. Res. 44*, 83−90.

(4) Kobayashi, H., Longmire, M. R., Ogawa, M., and Choyke, P. L. (2011) Rational chemical design of the next generation of molecular imaging probes based on physics and biology: mixing modalities, colors and signals. *Chem. Soc. Rev. 40*, 4626−4648.

(5) Kobayashi, H., Ogawa, M., Alford, R., Choyke, P. L., and Urano, Y. (2010) New strategies for fluorescent probe design in medical diagnostic imaging. *Chem. Rev. 110*, 2620−2640.

(6) Hilderbrand, S. A., and Weissleder, R. (2010) Near-infrared fluorescence: application to in vivo molecular imaging. *Curr. Opin. Chem. Biol. 14*, 71−79.

(7) Weissleder, R., and Pittet, M. J. (2008) Imaging in the era of molecular oncology. *Nature 452*, 580−589.
(8) Kobayashi, H., Hama, Y., Koyama, Y., Barrett, T., Regino, C. A., Urano, Y., and Choyke, P. L. (2007) Simultaneous multicolor imaging of five different lymphatic basins using quantum dots. *Nano Lett. 7*, 1711−1716.
(9) Koyama, Y., Barrett, T., Hama, Y., Ravizzini, G., Choyke, P. L., and Kobayashi, H. (2007) In vivo molecular imaging to diagnose and subtype tumors through receptor-targeted optically labeled monoclonal antibodies. *Neoplasia 9*, 1021−1029.
(10) Kobayashi, H., Ogawa, M., Kosaka, N., Choyke, P. L., and Urano, Y. (2009) Multicolor imaging of lymphatic function with two nanomaterials: quantum dot-labeled cancer cells and dendrimer-based optical agents. *Nanomedicine 4*, 411−419.
(11) Lindsey, J. S., Mass, O., and Chen, C.-Y. (2011) Tapping the near infrared spectral region with bacteriochlorin arrays. *New J. Chem. 35*, 511−516.
(12) Grimm, B., Porra, R. J., Rüdiger, W., and Scheer, H. (2006) Chlorophylls and Bacteriochlorophylls. Biochemistry, Biophysics, Function and Applications, in *Advances in Photosynthesis and Respiration* (Scheer, H., Ed.) Springer, Dodrecht, The Netherlands.
(13) Brückner, C., Samankumara, L., and Ogikubo, J. (2012) Syntheses of Bacteriochlorins and Isobacteriochlorins, in *Handbook of Porphyrin Sciences*, vol 17, (Kadish, K. M., Smith, K. M., and Guilard, R., Eds.) pp 1−112, World Scientific, River Edge, NY.
(14) Yang, E., Kirmaier, C., Krayer, M., Taniguchi, M., Kim, H. J., Diers, J. R., Bocian, D. F., Lindsey, J. S., and Holten, D. (2011) Photophysical properties and electronic structure of stable, tunable synthetic bacteriochlorins: extending the features of native photosynthetic pigments. *J. Phys. Chem. B 115*, 10801−10816.
(15) Taniguchi, M., Cramer, D. L., Bhise, A. D., Kee, H. L., Bocian, D. F., Holten, D., and Lindsey, J. S. (2008) Accessing the near-infrared spectral region with stable, synthetic, wavelength-tunable bacteriochlorins. *New J. Chem. 32*, 947−958.
(16) Cao, W., Ng, K. K., Corbin, I., Zhang, Z., Ding, L., Chen, J., and Zheng, G. (2009) Synthesis and evaluation of a stable bacteriochlorophyll-analog and its incorporation into high-density lipoprotein nanoparticles for tumor imaging. *Bioconjugate Chem. 20*, 2023−2031.
(17) Liu, T. W., Chen, J., Burgess, L., Cao, W., Shi, J., Wilson, B. C., and Zheng, G. (2011) Multimodal bacteriochlorophyll theranostic agent. *Theranostics 1*, 354−362.
(18) Ptaszek, M., Kee, H. L., Muthiah, C., Nothdurft, R., Akers, W., Achilefu, S., Culver, J. P., and Holten, D. (2010) Near-infrared molecular imaging probes based on chlorin-bacteriochlorin dyads. *Proc. SPIE 7576E*, 1−9.
(19) Lovell, J. F., Jin, C. S., Huynh, E., Jin, H., Kim, C., Rubinstein, J. L., Chan, W. C., Cao, W., Wang, L. V., and Zheng, G. (2011) Porphysome nanovesicles generated by porphyrin bilayers for use as multimodal biophotonic contrast agents. *Nat. Mater. 10*, 324−332.
(20) Yu, Z., and Ptaszek, M. (2013) Near-IR emissive chlorin-bacteriochlorin energy-transfer dyads with a common donor and acceptors with tunable emission wavelength. *J. Org. Chem. 78*, 10678−10691.
(21) Ogawa, M., Kosaka, N., Choyke, P. L., and Kobayashi, H. (2009) H-type dimer formation of fluorophores: a mechanism for activatable, in vivo optical molecular imaging. *ACS Chem. Biol. 4*, 535−546.
(22) Ogawa, M., Kosaka, N., Choyke, P. L., and Kobayashi, H. (2009) In vivo molecular imaging of cancer with a quenching near-infrared fluorescent probe using conjugates of monoclonal antibodies and indocyanine green. *Cancer Res. 69*, 1268−1272.
(23) Sutton, J. M., Clarke, O. J., Fernandez, N., and Boyle, R. W. (2002) Porphyrin, chlorin, and bacteriochlorin isothiocyanates: useful reagents for the synthesis of photoactive bioconjugates. *Bioconjugate Chem. 13*, 249−263.
(24) Sutton, J. M., Fernandez, N., and Boyle, R. W. (2000) Functionalized diphenylchlorins and bacteriochlorins: their synthesis and bioconjugation for targeted photodynamic therapy and tumor imaging. *J. Porphyrins Phthalocyanines 4*, 655−658.
(25) Springer, J. W., Parkes-Loach, P. S., Reddy, K. R., Krayer, M., Jiao, J., Lee, G. M., Niedzwiedzki, D. M., Harris, M. A., Kirmaier, C., Bocian, D. F., Lindsey, J. S., Holten, D., and Loach, P. A. (2012) Biohybrid photosynthetic antenna complexes for enhanced light-harvesting. *J. Am. Chem. Soc. 134*, 4589−4599.
(26) Reddy, K. R., Jiang, J., Krayer, M., Harris, M. A., Springer, J. W., Yang, E., Jiao, J., Niedzwiedzki, D. M., Pandithavidana, D., Parkes-Loach, P. S., Kirmaier, C., Loach, P. A., Bocian, D. F., Holten, D., and Lindsey, J. S. (2013) Palette of lipophilic bioconjugatable bacteriochlorins for construction of biohybrid light-harvesting architectures. *Chem. Sci. 4*, 2036−2053.
(27) McCarthy, J. R., Bhaumik, J., Merbouh, N., and Weissleder, R. (2009) High-yielding syntheses of hydrophilic conjugatable chlorins and bacteriochlorins. *Org. Biomol. Chem. 7*, 3430−3436.
(28) Regino, C. A., Ogawa, M., Alford, R., Wong, K. J., Kosaka, N., Williams, M., Feild, B. J., Takahashi, M., Choyke, P. L., and Kobayashi, H. (2010) Two-step synthesis of galactosylated human serum albumin as a targeted optical imaging agent for peritoneal carcinomatosis. *J. Med. Chem. 53*, 1579−1586.
(29) Hama, Y., Urano, Y., Koyama, Y., Kamiya, M., Bernardo, M., Paik, R. S., Shin, I. S., Paik, C. H., Choyke, P. L., and Kobayashi, H. (2007) A target cell-specific activatable fluorescence probe for in vivo molecular imaging of cancer based on a self-quenched avidin-rhodamine conjugate. *Cancer Res. 67*, 2791−2799.
(30) Gunn, A. J., Hama, Y., Koyama, Y., Kohn, E. C., Choyke, P. L., and Kobayashi, H. (2007) Targeted optical fluorescence imaging of human ovarian adenocarcinoma using a galactosyl serum albumin-conjugated fluorophore. *Cancer Sci. 98*, 1727−1733.
(31) Hama, Y., Urano, Y., Koyama, Y., Choyke, P. L., and Kobayashi, H. (2006) Targeted optical imaging of cancer cells using lectin-binding BODIPY conjugated avidin. *Biochem. Biophys. Res. Commun. 348*, 807−813.
(32) Kosaka, N., Ogawa, M., Paik, D. S., Paik, C. H., Choyke, P. L., and Kobayashi, H. (2010) Semiquantitative assessment of the microdistribution of fluorescence-labeled monoclonal antibody in small peritoneal disseminations of ovarian cancer. *Cancer Sci 101*, 820−825.
(33) Hama, Y., Urano, Y., Koyama, Y., Choyke, P. L., and Kobayashi, H. (2007) D-galactose receptor-targeted in vivo spectral fluorescence imaging of peritoneal metastasis using galactosamin-conjugated serum albumin-rhodamine green. *J. Biomed. Opt. 12*, 051501.
(34) Alexander, V. M., Sano, K., Yu, Z., Nakajima, T., Choyke, P. L., Ptaszek, M., and Kobayashi, H. (2012) Galactosyl human serum albumin-NMP1 conjugate: a near infrared (NIR)-activatable fluorescence imaging agent to detect peritoneal ovarian cancer metastases. *Bioconjugate Chem. 23*, 1671−1679.